

Localization-delocalization transitions in a two-dimensional quantum percolation model: von Neumann entropy studies

Longyan Gong^{1,*} and Peiqing Tong^{2,†}

¹*Center of Optofluidic Technology and College of Science, Nanjing University of Posts and Telecommunications, Nanjing 210003, China*

²*Department of Physics, Nanjing Normal University, Nanjing 210097, China*

(Received 10 July 2009; revised manuscript received 15 October 2009; published 20 November 2009)

In two-dimensional quantum site-percolation square lattice models, the von Neumann entropy is extensively studied numerically. At a certain eigenenergy, the localization-delocalization transition is reflected by the derivative of von Neumann entropy which is maximal at the quantum percolation threshold p_q . The phase diagram of localization-delocalization transitions is deduced in the extrapolation to infinite system sizes. The nonmonotonic eigenenergies dependence of p_q and the lowest value $p_q \approx 0.665$ are found. At localized-delocalized transition points, the finite scaling analysis for the von Neumann entropy is performed and it is found the critical exponents ν not to be universal. These studies provide an evidence that the existence of a quantum percolation threshold $p_q < 1$ in the two-dimensional quantum percolation problem.

DOI: [10.1103/PhysRevB.80.174205](https://doi.org/10.1103/PhysRevB.80.174205)

PACS number(s): 71.30.+h, 03.67.-a, 72.15.Rn

I. INTRODUCTION

The Anderson model^{1,2} and the quantum percolation (QP) model^{3,4} are two important theoretical models that are used to study electron localization properties in disordered systems. In the two models, the on-site energy randomness and the geometric randomness are considered, respectively. For the Anderson model, there are extensive studies and definitive results,² while for the QP model, there are many open issues even today.

The main concern in QP problems is to locate the QP threshold p_q (accessible site concentrations by quantum particles) below which the electron is localized with probability one. For the Anderson model and the QP model, there is a consensus on the existence of localization-delocalization transitions (LDTs) in three dimensions (3D).⁵⁻⁸ For Anderson models, according to the one-parameter scaling theory,⁹ LDTs do not occur at and below two dimensions (2D). However, whether the scaling theory is suitable for the QP model is an open question¹⁰ and even whether LDTs exist in 2D QP models at $p_q < 1$ is less clear.¹¹ Studies such as the scaling work based on numerical calculations of the conductance¹² and transfer matrix methods with finite-size scaling analysis¹³ showed no evidence for LDTs. At the same time, there are many studies that claim LDTs exist.¹⁴⁻¹⁸ However, the values of QP threshold p_q obtained by different methods are not consistent. For example, for 2D quantum site-percolation square lattice models, Odagaki *et al.*, obtained $p_q \approx 0.59$ by a Green's function method.¹⁴ Koslowski and von Niessen gave $p_q \approx 0.70$ with the Thouless number based on the Thouless-Edwards-Licciardello method.¹⁵ Srivastava and Chaturvedi showed $p_q \approx 0.73$ with the participation used by the method with equations of motion.¹⁶ Odagaki and Chang found $p_q \approx 0.87$ using a real-space renormalization-group method.¹⁷ Raghavan obtained $p_q \approx 0.95$ by mapping a 2D system into a one-dimensional system.¹⁸ Very recently, Islam and Nakanishi suggested that p_q depending on particle energies by calculating the transmission coefficient for 2D bond-percolation models.¹¹

In the mean time, metal states or metal-insulator transitions are observed experimentally in a variety of dilute two-

dimensional electron and hole systems.¹⁹ At the same time, the unusual transport properties of materials,¹⁰ such as metal-insulator transitions happen in perovskite manganite films²⁰ and in granular metals,²¹ and minimal conductivity in undoped graphenes,²² may be explained by 2D QP models. Therefore these give additional motivations to study LDTs in 2D QP models.

On the other hand, quantum entanglement, which attracts much attention in quantum information,²³ has been extensively applied in condensed matter physics.^{7,25-34} For example, quantum entanglement measured by the von Neumann entropy was studied in the extended Hubbard model,^{26,27} in quantum small-world networks,²⁹ in two interacting particle systems,³⁰ in the extended Harper model,^{27,31} in three dimensional Anderson models,³² in the integer quantum Hall system,³² and in spin models.^{33,34} It is found that the von Neumann entropy shows singular behaviors at quantum critical points (QCPs). The derivative of von Neumann entropy has very good finite-size scaling behaviors close to QCPs even for quite small system sizes.³²⁻³⁴ Therefore it becomes a powerful method to quantify QCPs in various systems.

In this paper, with the help of the von Neumann entropy we present a detailed numerical study of LDTs in the 2D quantum site-percolation model. Our studies show that a quantum site-percolation threshold $p_q < 1$ exists in the 2D QP problem. In the next section the QP model and the definition of von Neumann entropy are introduced. In Sec. III the numerical results are presented. And we present our conclusions and discussions in Sec. IV.

II. QUANTUM SITE-PERCOLATION MODEL AND VON NEUMANN ENTROPY

A. Quantum site-percolation model

Let us consider one-electron tight-binding Hamiltonian with diagonal disorder defined on square lattices of sites¹⁰

$$H = \sum_i \xi_i c_i^\dagger c_i - t \sum_{\langle ij \rangle} (c_i^\dagger c_j + H.c.), \quad (1)$$

where ξ_i is on-site potential, t is a nearest-neighbor hopping integral, and c_i^\dagger (c_i) is creation (annihilation) operators of the i th site. The on-site potential ξ_i can be drawn from the bimodal distribution

$$p(\xi_i) = p\delta(\xi_i - \xi_A) + (1-p)\delta(\xi_i - \xi_B). \quad (2)$$

In the limit $\xi_B - \xi_A \rightarrow \infty$, the electron moves only on a random assembly of A -lattice points. Without loss of generality we choose $\xi_A = 0$. In the situation the A -site occupation probability is p and the corresponding quantum site-percolation Hamiltonian reads

$$H_{AA} = -t \sum_{\langle ij \rangle \in A} (c_i^\dagger c_j + H.c.), \quad (3)$$

where the summation extends over nearest-neighbor A sites only.

B. von Neumann entropy

The general definition of entanglement is based on the von Neumann entropy.²⁴ The generic eigenstate $|\alpha\rangle$ of Hamiltonian (3) with eigenenergy ε_α is the superposition

$$|\alpha\rangle = \sum_{i \in A} \psi_i^\alpha |i\rangle = \sum_{i \in A} \psi_i^\alpha c_i^\dagger |0\rangle, \quad (4)$$

where $|0\rangle$ is the vacuum and ψ_i^α is the amplitude of wave function at i th site. For an electron in the system, there are two local states at each site, i.e., $|1\rangle_i$ and $|0\rangle_i$, corresponding to the state with (without) an electron at the i th site, respectively. The local density matrix ρ_i is defined^{25,26,29-32} by

$$\rho_i = z_i |1\rangle_i \langle 1| + (1 - z_i) |0\rangle_i \langle 0|, \quad (5)$$

where $z_i = \langle \alpha | c_i^\dagger c_i | \alpha \rangle = |\psi_i^\alpha|^2$ is the local occupation number at i th site. Consequently, the corresponding von Neumann entropy related to the i th site is

$$E_{vi}^\alpha = -z_i \log_2 z_i - (1 - z_i) \log_2 (1 - z_i). \quad (6)$$

For nonuniform systems, the value of E_{vi}^α depends on the site position i . At an eigenstate α , we define a site-averaged von Neumann entropy

$$E_v^\alpha = \frac{1}{N} \sum_{i=1}^N E_{vi}^\alpha, \quad (7)$$

where N is the number of A -lattice sites. The definition (7) shows that for an extended state that $\psi_i^\alpha = \frac{1}{\sqrt{N}}$ for all i , $E_v^\alpha = -\frac{1}{N} \log_2 \frac{1}{N} - (1 - \frac{1}{N}) \log_2 (1 - \frac{1}{N}) \approx \frac{1}{N} \log_2 N$ at $N \rightarrow \infty$, and for a localized state that $\psi_i^\alpha = \delta_{i i_0}$ (i_0 is a given site), $E_v^\alpha = 0$. In the present paper all the values of E_v^α is scaled by $\frac{1}{N} \log_2 N$. From the two examples, we know the scaled E_v^α is near 1 when eigenstates are extended and near zero when eigenstates are localized. Henceforth, we omit ‘‘scaled’’ for simplicity.

For a random system the site-averaged von Neumann entropy E_v^α should be further averaged over different realiza-

tions of disorder. The resulting quantity, the disorder averaged von Neumann entropy denoted by $\langle E_v^\alpha \rangle$ for eigenenergy ε_α , which is defined as

$$\langle E_v^\alpha \rangle = \overline{\frac{1}{N} \sum_{i=1}^N E_{vi}^\alpha} = \frac{1}{K} \frac{1}{N} \sum_{i=1}^N E_{vi}^\alpha, \quad (8)$$

where $\bar{}$ is denoted as random average and K is the number of disorder realizations. In practice, $\langle E_v^\alpha \rangle$ is the average values over a small window Δ around an energy value ε , i.e., $\varepsilon_\alpha \in [\varepsilon - \Delta/2, \varepsilon + \Delta/2]$. We ensure that Δ is sufficiently small, and at the same time there are enough states in the interval Δ . Here $\Delta = 0.04$ is chosen and other Δ give similar results.

Another quantitative measure that is widely used to characterize localization is the participation ratio (PR),³⁵ defined by $\xi_\alpha = (N \sum_{i=1}^N |\psi_i^\alpha|^4)^{-1}$, which gives the ratio of lattice sites

occupied by particles to all lattice sites at an eigenstate α . For the above extended and fully localized states, $\xi_\alpha = 1$ and $1/N$, respectively. Generally speaking, the larger ξ_α is, the more delocalized the eigenstate is. Similarly, the disorder averaged PR $\langle \xi_\alpha \rangle$ is also averaged over the same small energy window. Henceforth, the disorder averaged von Neumann entropy $\langle E_v^\alpha \rangle$ and the disorder averaged PR $\langle \xi_\alpha \rangle$ are simplified to the von Neumann entropy $\langle E_v^\alpha \rangle$ and the PR $\langle \xi_\alpha \rangle$, respectively.

III. NUMERICAL RESULTS

In numerical calculations, we directly diagonalize the eigenvalue Eq. (3) with the periodic boundary condition and obtain all eigenvalues ε_α and the corresponding eigenstates $|\alpha\rangle$. Without loss of generality, the hopping integral t is taken as units of energy. From formulas (6)–(8), we can obtain the von Neumann entropy $\langle E_v^\alpha \rangle$. We consider systems of linear size $L = 20, 30, \dots, 60$ (measured in units of the lattice constant) and having $N = L^2$ A -lattice sites in total. The corresponding number of disorder realizations $K = 2500, 2000, \dots, 500$, respectively. More realizations give similar results.

Before discussing possible localized-delocalized transitions let us investigate the behavior of the von Neumann entropy $\langle E_v^\alpha \rangle$ at different site occupation probability p . The $\langle E_v^\alpha \rangle$ as functions of eigenenergies ε_α are plotted in Figs. 1(a)–1(c) at $L = 20, 40$ and 60 for $p = 0.2, 0.7$ and 0.9 , respectively. It shows that at the same p , the values of $\langle E_v^\alpha \rangle$ depend on eigenenergies ε_α and system sizes L . For $p = 0.7$ and 0.9 , the $\langle E_v^\alpha \rangle$ are relatively small for eigenstates near the band edges, while relatively large for eigenstates near the band center except eigenstates very near the band edges. Comparing the values of $\langle E_v^\alpha \rangle$ for the three p at the same L , on the whole, all $\langle E_v^\alpha \rangle$ are relatively small for $p = 0.2$ and relatively large for $p = 0.9$. Compared to our results, the PR are also plotted in Fig. 1(d) for $L = 60$ at the three p . The variations of the PR $\langle \xi_\alpha \rangle$ with respect to ε_α are similar to that of $\langle E_v^\alpha \rangle$ in Figs. 1(a)–1(c). At the same time, the $\langle E_v^\alpha \rangle$ versus the corresponding $\langle \xi_\alpha \rangle$ are plotted in Fig. 2. It shows that the $\langle E_v^\alpha \rangle$

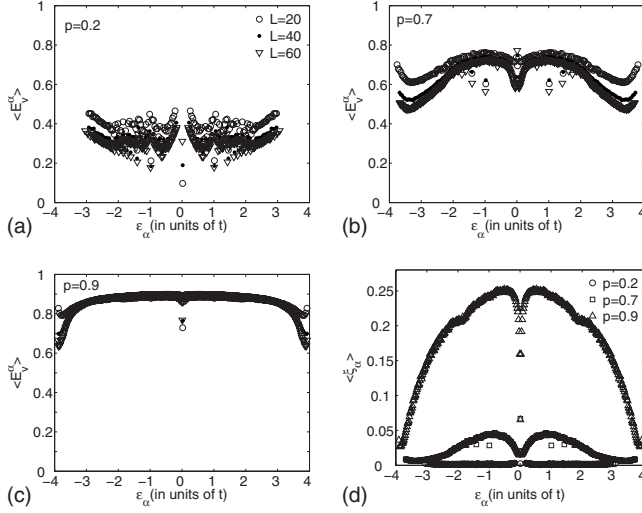


FIG. 1. The von Neumann entropy $\langle E_v^\alpha \rangle$ varying with eigenenergies ε_α at $L=20, 40$, and 60 for site occupation probability (a) $p=0.2$, (b) $p=0.7$, and (c) $p=0.9$, respectively. (d) The corresponding PR $\langle \xi_\alpha \rangle$ at $p=0.2, 0.7$, and 0.9 for $L=60$.

increases monotonously with the $\langle \xi_\alpha \rangle$, so the von Neumann entropy can reflect the localization properties of eigenstates in the QP model. To demonstrate the localization properties intuitively, five typical wave function amplitude distributions are plotted in Figs. 3(a)–3(e). For $p=0.2$, all eigenstates are localized in spaces like that shown in Fig. 3(a). For $p=0.9$, almost all eigenstates are extended similarly to that in Fig. 3(e). For $p=0.7$, there are localized states [Fig. 3(b)] and delocalized states [Figs. 3(c) and 3(d)]. As illustrated in the caption of Fig. 3, the values of E_v^α and ξ_α are relatively large for extended or delocalized states and relatively small for localized states, respectively.

To get a more detailed picture, a typical $\langle E_v^\alpha \rangle$ varying with all ε_α and p for $L=60$ is plotted in Fig. 4. The line of mobility edges computed in Ref. 15 is also plotted the figure. The extended (localized) region is above (below) the line. Figure 4 shows that, except at the band center, the $\langle E_v^\alpha \rangle$ are large and small for the regions above and below the line of mobility edges, relatively, and abruptly changes at the line. All these mean the $\langle E_v^\alpha \rangle$ can reflect the localized-delocalized transitions in the model.

To exact locate localized-delocalized transition points and the corresponding critical exponents with a finite-size scaling

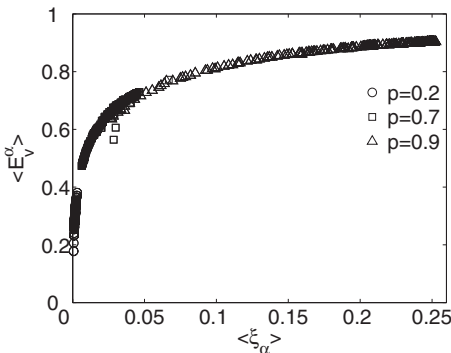


FIG. 2. The relation between the $\langle E_v^\alpha \rangle$ and the corresponding PR $\langle \xi_\alpha \rangle$ at $L=60$ for states shown in Fig. 1.

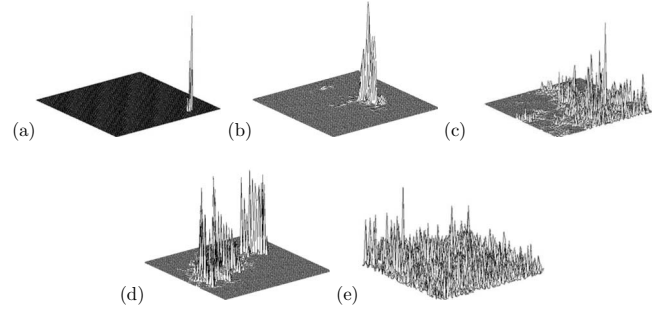


FIG. 3. Amplitude distributions of some eigenfunctions for $L=60$. (a) $\varepsilon_\alpha=-0.8349$, $E_v^\alpha=0.3167$, and $\xi_\alpha=0.0016$ for $p=0.2$. (b) $\varepsilon_\alpha=-2.7867$, $E_v^\alpha=0.5586$, and $\xi_\alpha=0.0103$, (c) $\varepsilon_\alpha=-0.6568$, $E_v^\alpha=0.8424$, and $\xi_\alpha=0.1318$, and (d) $\varepsilon_\alpha=-0.1291$, $E_v^\alpha=0.6842$, and $\xi_\alpha=0.0352$ for $p=0.7$. (e) $\varepsilon_\alpha=-0.5179$, $E_v^\alpha=0.9221$, and $\xi_\alpha=0.3393$ for $p=0.9$.

analysis, in the follows, we study the von Neumann entropy $\langle E_v^\alpha \rangle$ changes with the site occupation probability p for different eigenenergies. We found that the general trend for all von Neumann entropy $\langle E_v^\alpha \rangle$ curves at different eigenenergies are similar except the one at the band center, so we will discuss only two energies as examples, one that is away from the band center and one very close to the band center.

A. Eigenenergies away from the band center

We first study the von Neumann entropy $\langle E_v^\alpha \rangle$ and related quantities for eigenstates with eigenenergies $\varepsilon_\alpha \in [-0.84-0.02, -0.84+0.02]$. The literatures^{11,14–17} agree on the QP threshold $p_q \geq p_c \approx 0.593$ if p_q exits, where p_c is the classical percolation threshold.³⁶ Therefore, we study the QP model at the site occupation probability p beginning from 0.4 , which is far smaller than the lower bound of p_q .

In Fig. 5(a), we show the dependence of $\langle E_v^\alpha \rangle$ on the site occupation probability p at system sizes $L=20, 30, \dots, 60$, respectively. It shows that $\langle E_v^\alpha \rangle$ monotonically increases as p becomes larger. For a certain system size, when p is small, e.g., $p=0.4$, the eigenstates are localized and $\langle E_v^\alpha \rangle$ is small. When $p=1.0$, the model shown in Eq. (3) is a two-dimensional periodic potential system. Due to the Bloch

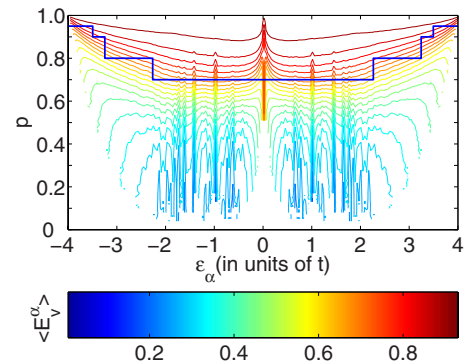


FIG. 4. (Color online) The von Neumann entropy $\langle E_v^\alpha \rangle$ varying with eigenenergies ε_α and the site occupation probability p at $L=60$. Line: mobility edge trajectory obtained by Koslowski and von Niessen. (Ref. 15)

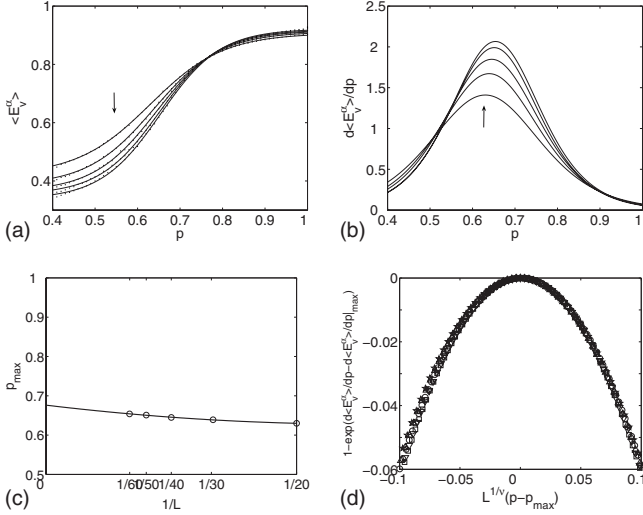


FIG. 5. Some quantities for eigenstates with eigenenergies $\varepsilon_\alpha \in [-0.84 - 0.02, -0.84 + 0.02]$. (a) The von Neumann entropy $\langle E_v^\alpha \rangle$ varying with the site occupation probability p and the lines are Boltzmann fitting. (b) The derivative $d\langle E_v^\alpha \rangle/dp$ varying with p . (c) The line corresponds to the expected behavior of p_{max} for $1/L \rightarrow 0$ according to a second-order polynomial fitting. (d) The finite-size scaling analysis. The system sizes $L=20, 30, \dots, 60$ and the arrow direction in (a) and (b) denotes the increasing of L .

theorem the eigenstate of a tight-binding electron on a local regular lattice is always in the extended state. At the situation, $\langle E_v^\alpha \rangle$ is largest. All these reflect the trivial delocalization effect of p , which is similar as that studied in quantum small-world network models.²⁹ All data shown in Fig. 5(a) are well fitted with nonlinear Boltzmann functions for various system sizes. According to the fitted lines, we plot the derivative $d\langle E_v^\alpha \rangle/dp$ varying with p in Fig. 5(b). It shows there is a peak in the derivative at a certain p , which is denoted by p_{max} . The maximal derivative and p_{max} increase with the system sizes L , respectively. It is believed that the von Neumann entropy may be nonanalytic at a quantum phase transitions and can reflect various quantum critical points.^{26,32} Therefore, that the derivative is maximal at a certain position p_{max} , can be as a signature of LDTs of electron states.^{27,29}

To study the LDTs at the QP threshold p_q , one needs to investigate the behavior of systems in the thermodynamic limit. However, in most cases this is not possible in numerical methods,³⁷ and therefore, similarly as in Ref. 27 an extrapolation method is chosen. Figure 5(c) shows the scaling behavior of the p_{max} . The p_q in the thermodynamic limit can be obtained by $1/L \rightarrow 0$ and Fig. 5(c) shows $p_q \approx 0.676$ at the situation. We denote the derivative of von Neumann entropy at p_{max} as $d\langle E_v^\alpha \rangle/dp|_{max}$. Following the Refs. 33 and 34, the finite-size scaling is performed for the function $1 - \exp(d\langle E_v^\alpha \rangle/dp - d\langle E_v^\alpha \rangle/dp|_{max})$ with respect to $L^{1/\nu}(p - p_{max})$. The result is presented in Fig. 5(d). It shows numerical results obtained from various system sizes approximately collapse on a single curve with the critical exponent $\nu \approx 2.52$.

B. Eigenenergies near the band center

In the following, we discuss the von Neumann entropy $\langle E_v^\alpha \rangle$ for eigenstates with eigenenergies ε_α

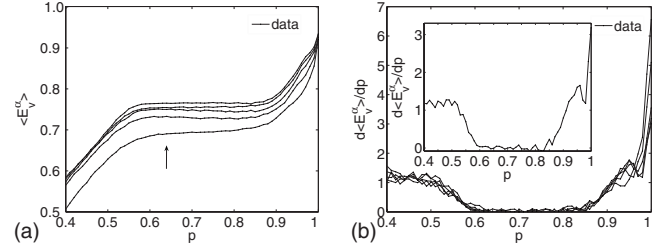


FIG. 6. Some quantities for eigenstates with eigenenergies $\varepsilon_\alpha \in [0 - 0.02, 0 + 0.02]$. (a) The von Neumann entropy $\langle E_v^\alpha \rangle$ and (b) the $d\langle E_v^\alpha \rangle/dp$ varying with the site occupation probability p . The system sizes $L=20, 30, \dots, 60$ and the arrow direction in (a) and (b) denotes the increasing of L . The inset in (b) is for $L=60$.

$\varepsilon_\alpha \in [0 - 0.02, 0 + 0.02]$. The von Neumann entropy $\langle E_v^\alpha \rangle$ and the corresponding derivative $d\langle E_v^\alpha \rangle/dp$ varying with the site occupation probability p are shown in Figs. 6(a) and 6(b), respectively. Figure 6(a) shows that $\langle E_v^\alpha \rangle$ first increases with p until to a plateau at $p \in [0.6, 0.85]$, then continues to increase, which is quite different from that shown in Fig. 5(a) for eigenenergies away from the band center. Figure 6(b) shows that the derivative $d\langle E_v^\alpha \rangle/dp$ drastically decreases near $p \approx 0.6$ and drastically increases near $p \approx 0.85$.

With a real-space renormalization-group method, Odagaki and Chang observed three regimes of the electronic properties in QP models, which divided by the classical percolation threshold p_c and the quantum percolation threshold p_q ($p_q > p_c$).¹⁷ When $p < p_c$, electrons cannot tunnel between different isolated clusters and electrons are considered to be localized in the classical sense even in the quantum case. When $p_c < p < p_q$, due to quantum interference effects, electrons cannot spread infinitely even there is an infinitely extended channel. The regime is called quantum localization regimes. When $p > p_q$, electrons can spread infinitely and electron states are extended. They found $p_c = 0.618$ and $p_q = 0.867$. It is interesting that the von Neumann entropy $\langle E_v^\alpha \rangle$ drastically changes near the two p values.

C. Phase diagram

We have studied and extensively analyzed the von Neumann entropy for all the other eigenstates. As the system in Eq. (3) is bipartite, ε_α and $-\varepsilon_\alpha$ are both eigenvalues of \hat{H}_{AA} .¹⁵ Therefore we will restrict our investigation to one (left) half side of the band, i.e., $-4 < \varepsilon_\alpha < 0$. Figure 7(a) presents the phase diagram of LDTs in the $\varepsilon_\alpha - p$ plane. The values of p at the LDTs are the QP threshold p_q , which is obtained by the extrapolation method similarly as that shown in Fig. 5(c). The trend for p_q varying with ε_α is similar as that for 2D quantum bond-percolation models on square lattices¹¹ and 3D quantum site-percolation models on simple cubic lattice.^{5,8} In detail, we observe the nonmonotonic dependence of the values of p_q on eigenenergies ε_α . Notice that in the region $-2t < \varepsilon_\alpha < -0.5t$ the QP threshold p_q are nearly constant and a weak maximum at $\varepsilon_\alpha \approx -t$, which are very similar as that found in Ref. 5. That a weak maximum for p_q at $\varepsilon_\alpha \approx -t$ has also been found and discussed in Ref. 8, which may be due to the existence of von Hove singularity at the

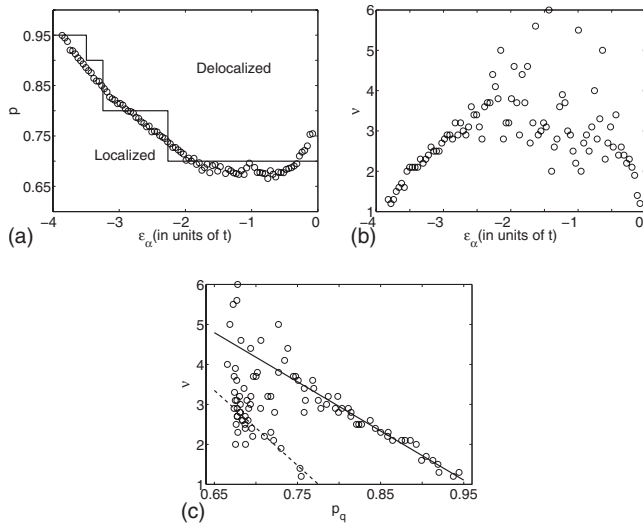


FIG. 7. (a) The phase diagram of LDTs in the space of eigenenergies ε_α and the site occupation probability p . The values of p at the LDTs are QP threshold p_q . Line: mobility edge trajectory obtained by Koslowski and von Niessen. (Ref. 15) (b) The critical exponents ν versus eigenenergies ε_α . (c) The critical exponents ν versus QP threshold p_q . The solid line and the dashed line are the best linear fitting for $\varepsilon_\alpha < -2.0t$ and $\varepsilon_\alpha > -0.5t$, respectively.

energy.⁵ We find all the QP threshold p_q are greater than the classical percolation threshold $p_c \approx 0.593$ and the lowest value $p_q \approx 0.665$. As shown in Fig. 7(a), the phase diagram is very consistent with the mobility edge trajectory shown in Ref. 15 for the same model obtained by the Thouless-Edwards-Licciardello method.

Figure 7(b) presents all the critical exponents ν versus eigenenergies ε_α according to the finite scaling analysis similarly as that shown in Fig. 5(d). We find the values of ν depend on eigenenergies ε_α . In detail, in the region $-2t < \varepsilon_\alpha < -0.5t$ where p_q are almost constant [see Fig. 7(a)], most of the values of ν are distributed in a relatively narrow interval [2.6, 3.2]. From the band edge to $\varepsilon_\alpha \approx -2t$, ν increase with ε_α , while from $\varepsilon_\alpha \approx -0.5t$ to the band center, ν decrease with ε_α . All ν are larger than $2/D$ ($D=2$), which satisfies the assumption that ν must satisfy the bound $\nu \geq 2/D$ for random systems.³⁸ Though ν has been extensively studied in 3D QP models,^{6,7,17} to our best knowledge, there are few works to study ν in 2D QP models except in Ref. 17, where the critical exponent for correlation lengths $\nu \approx 3.35$. The varying of the critical exponent ν with the QP threshold p_q is plotted in Fig. 7(c). It shows near the band edge and near the band center the relation between ν and p_q is linear, respec-

tively, but the linear relations are different. This may be caused by the different symmetry and/or degeneration at the two energy regions.^{3,8}

IV. CONCLUSIONS AND DISCUSSIONS

In this paper, we have detailed studied the von Neumann entropy $\langle E_v^\alpha \rangle$ varying with eigenenergies ε_α and accessible site concentrations p by quantum particles in two-dimensional quantum site-percolation models on square lattices.

For eigenenergies away from the band center, we determine the QP threshold p_q by the derivative of von Neumann entropy is maximal at the point. Based on this, we give the phase diagram of LDTs in the ε_α - p plane, which is very consistent with the mobility edge trajectory shown in Ref. 15. From the phase diagram, we observe the nonmonotonic eigenenergies dependence of p_q and the lowest value $p_q \approx 0.665$. At the same time, the finite-size scaling analysis is performed at all LDTs points. To the best of our knowledge, it is the first time to obtain all the critical exponents ν at the whole energy space for 2D QP models. We find the critical exponents ν depend on eigenenergies ε_α .

For eigenenergies near the band center, the variations of the von Neumann entropy $\langle E_v^\alpha \rangle$ with respect to p for are quite different from that for eigenenergies away from the band center. It can reflect the classical percolation threshold p_c and the QP threshold p_q for eigenenergies at the band center.

All our numerical results show that there is $p_q < 1$ in 2D QP models and p_q depends on eigenenergies. The debates on the values of p_q may be partially due to different energies treated in literatures.

ACKNOWLEDGMENTS

This project was supported by the National Natural Science Foundation of China (Grants No. 10674072 and No. 10974097), by the Specialized Research Fund for the Doctoral Program of Higher Education (Grant No. 20060319007), and by National Key Projects for Basic Research of China (Grant No. 2009CB929501). L.G. is supported in part by the National Natural Science Foundation of China (Grants No. 10904047), by the Nature Science Foundation of Jiangsu Province of China (Grant No. 08KJB140005) and by the Specialized Research Fund for the Doctoral Program of Higher Education (Grant No. 20060293001).

*lygong@njupt.edu.cn

†Corresponding author; pqtong@njnu.edu.cn

¹P. W. Anderson, Phys. Rev. **109**, 1492 (1958).

²F. Evers and A. D. Mirlin, Rev. Mod. Phys. **80**, 1355 (2008).

³S. Kirkpatrick and T. P. Eggarter, Phys. Rev. B **6**, 3598 (1972).

⁴Percolation Structures and Processes, edited by G. Deutscher, R.

Zallen, and J. Adler (Adam Hilger, Bristol, England, 1983).

⁵C. M. Soukoulis, E. N. Economou, and G. S. Grest, Phys. Rev. B **36**, 8649 (1987).

⁶Th. Koslowski and W. von Niessen, Phys. Rev. B **44**, 9926 (1991).

⁷R. Berkovits and Y. Avishai, Phys. Rev. B **53**, R16125 (1996).

- ⁸G. Schubert, A. Weiße, and H. Fehske, Phys. Rev. B **71**, 045126 (2005).
- ⁹E. Abrahams, P. W. Anderson, D. C. Licciardello, and T. V. Ramakrishnan, Phys. Rev. Lett. **42**, 673 (1979).
- ¹⁰G. Schubert and H. Fehske, Phys. Rev. B **77**, 245130 (2008).
- ¹¹M. F. Islam and H. Nakanishi, Phys. Rev. E **77**, 061109 (2008).
- ¹²Y. Avishai and J. M. Luck, Phys. Rev. B **45**, 1074 (1992).
- ¹³C. M. Soukoulis and G. S. Grest, Phys. Rev. B **44**, 4685 (1991).
- ¹⁴T. Odagaki, N. Ogita, and H. Matsuda, J. Phys. C **13**, 189 (1980).
- ¹⁵Th. Koslowski and W. von Niessen, Phys. Rev. B **42**, 10342 (1990).
- ¹⁶V. Srivastava and M. Chaturvedi, Phys. Rev. B **30**, 2238 (1984).
- ¹⁷T. Odagaki and K. C. Chang, Phys. Rev. B **30**, 1612 (1984).
- ¹⁸R. Raghavan, Phys. Rev. B **29**, 748 (1984).
- ¹⁹E. Abrahams, S. V. Kravchenko, and M. P. Sarachik, Rev. Mod. Phys. **73**, 251 (2001).
- ²⁰L. Zhang, C. Israel, A. Biswas, R. L. Greene, and A. de Lozanne, Science **298**, 805 (2002).
- ²¹M. V. Feigel'man, A. S. Ioselevich, and M. A. Skvortsov, Phys. Rev. Lett. **93**, 136403 (2004).
- ²²V. V. Cheianov, V. I. Falko, B. L. Altshuler, and I. L. Aleiner, Phys. Rev. Lett. **99**, 176801 (2007).
- ²³See, for example, *The Physics of Quantum Information* edited by D. Bouwmeester, A. Ekert, and A. Zeilinger (Springer, Berlin, 2000).
- ²⁴C. H. Bennett, H. J. Bernstein, S. Popescu, and B. Schumacher, Phys. Rev. A **53**, 2046 (1996).
- ²⁵P. Zanardi, Phys. Rev. A **65**, 042101 (2002).
- ²⁶S. J. Gu, S. S. Deng, Y. Q. Li, and H. Q. Lin, Phys. Rev. Lett. **93**, 086402 (2004).
- ²⁷C. Mund, Ö. Legeza, and R. M. Noack, Phys. Rev. B **79**, 245130 (2009).
- ²⁸Y. Chen, Z. D. Wang, and F. C. Zhang, Phys. Rev. B **73**, 224414 (2006).
- ²⁹L. Y. Gong and P. Q. Tong, Phys. Rev. E **74**, 056103 (2006).
- ³⁰L. Y. Gong and P. Q. Tong, Phys. Rev. B **76**, 085121 (2007).
- ³¹L. Y. Gong and P. Q. Tong, Phys. Rev. B **78**, 115114 (2008).
- ³²X. Jia, A. R. Subramaniam, I. A. Gruzberg, and S. Chakravarty, Phys. Rev. B **77**, 014208 (2008).
- ³³A. Osterloh, L. Amico, G. Falci, and R. Fazio, Nature (London) **416**, 608 (2002).
- ³⁴S. Q. Su, J. L. Song, and S. J. Gu, Phys. Rev. A **74**, 032308 (2006).
- ³⁵R. J. Bell and P. Dean, Discuss. Faraday Soc. **50**, 55 (1970).
- ³⁶D. Stauffer and A. Aharony, *Introduction to Percolation Theory*, 2nd ed. (Taylor & Francis, London, 1992).
- ³⁷M. A. Continentino, *Quantum Scaling in Many-Body Systems* (World Scientific, Singapore, 2001).
- ³⁸J. T. Chayes, L. Chayes, D. S. Fisher, and T. Spencer, Phys. Rev. Lett. **57**, 2999 (1986).